FINAL TECHNICAL
PROGRESS REPORT

CHEMISTRY

1. SYNTHESIS AND RECEPTOR AFFINITIES OF NEW 3-QUINUCLIDINYL ALPHA-HETEROARYL-ALPHA-ARYL-ALPHA-HYDROXYACETATES (see Schemes in App. 1.1). Five analogues of 3-quinuclidinyl benzilate were prepared in which one phenyl ring was substituted by a heterocycle; a bromine was included on either the remaining phenyl or the heterocycle to provide information relating to the affinity of potential radiohalogenated derivatives. The required methyl 4-bromophenylglyoxalate (1) was synthesized from the reaction between 4-bromophenylmagnesium bromide with an excess of dimethyl oxalate at -70° C. The reaction between ethyl oxalyl chloride with 2-bromothiphene provides ethyl 2-(5-bromothienyl)glyoxalate (2). Compounds (1) and (2) react with an equivalent amount of Grignard reagent to provide methyl or ethyl alpha-aryl-alpha-heteroarylglycolates (3). Transesterification of the methyl or ethyl esters (3) with (R,S)-3-quinuclidinol (4) in the presence of sodium metal provides the final products (5). As a result of screening the novel compounds, we found a heterocyclic derivative of QNB that may surpass IQNB as a CNS receptor radioligand. This novel compound binds to mAChRs with an affinity that is greater than that of IQNB, is selective for the m1 subtype, and is less lipophilic than IQNB, which should reduce the serum protein binding relative to IQNB. Cohen, Gibson, Fan, De La Cruz, Gitler, Hariman, Reba J. Pharm. Sci., 81, 326-329, 1992; App. 1.1.

2. SYNTHESIS AND STRUCTURE-ACTIVITY RELATIONSHIP OF SOME 5-[[[(DIALKYLAMINO)ALKYL]-1-PIPERIDINYL]ACETYL]-10,11-DIHYDRO-5H-DIBENZO[b,e][1,4]DIAZEPIN-11-ONES AS m2-SELECTIVE ANTIMUSCARINICS (see Schemes in App. 1.2). The required 11-oxo-10,11-dihydro-5H-dibenzo[b,e] [1,4]diazepine (9) was prepared from the reaction between 2-chlorobenzoic acid and o-phenylenediamine. The reaction between 2- and 4-vinylpyridines (5a,b) and dialkylamines (6a-e) provided 2- and 4-(dialkylamino)ethylpyridines (7). 4-Picolyllithium (5c) reacted with 3-(dimethyl- or diethylamino)propyl chloride to provide 4-[4-(dimethyl- or diethylamino)butyl]pyridines (7). [(Dialkylamino)alkyl]pyridines (7) were converted into the respective piperidines (8) by catalytic reduction(platinum oxide). Condensation of the tricycle (9) with chloroacetyl chloride provided 5-(chloroacetyl)-10,11-dihydro-5H-dibenzo[b,e][1,4] diazepin-11-one (10). Subsequent reaction with [(dialkylamino)alkyl]piperidines (8) yielded the final products (4). Compounds (4a-g,l,j) and two reference compounds (Table III in App. 1.2) were tested for their apparent affinities for the m1 and m2 subtypes. Table III compares the selectivity and potency of these compounds to other compounds. These data demonstrate that (4j) is the most potent compound in the series. This compound is selective for m2 receptors over m1 receptors by approximately 8-fold. These results also demonstrate that (4j) is approximately 10 times more potent at m2 receptors than AQ-RA 741. However, (4j) does not significantly penetrate the BBB. Cohen, Baumgold, Jin, de la Cruz, Rzeszotarski, Reba, J. Med. Chem. 36, 162-165, 1993a; App. 1.2.

3. SYNTHESIS OF SOME DIBENZODIAZEPINONES AS POTENT m2-SELECTIVE ANTIMUSCARINIC COMPOUNDS (see Schemes in App. 1.3). 4-[4-(Chloro)butyl]cyclohexylacetic acid (4) was obtained by catalytic reduction of 4-[4-(chloro)butyl]phenylacetic acid (3). Reaction of acid derivatives (4, 5) with thionyl chloride, followed by condensation with tricycle (6), and then reaction with secondary amines provided the final products (1, 2). To increase the lipophilicity in this series, we replaced the piperidine ring in the cationic head by cyclohexyl ring (Table I in App. 1.3). Compounds (1a-h), and (2a,b) and three reference compounds were tested for their apparent affinities for m1 and m2 subtypes. The IC_{50}'s for the muscarinic ligands were determined by competitive ligand binding assay against [^{3}H]QNB. These data demonstrate that (2b) is the most potent compound in the series. The data (Table III in App. 1.3.) reveal that neither preinjection nor coinjection of the m2-selective compound (2b) at a dose of 500 nmol or 2000 nmol affects the regional (R,R)-[^{125}I]IQNB accumulation in the rat brain. There was no displacement of (R,R)-[^{125}I]IQNB from specific brain regions by the unlabeled compound (2b). Cohen, Jin, Gitler, de la Cruz, Rzeszotarski, Zeeberg, Baumgold, Reba, J. Heterocyclic Chem. in press; App. 1.3.

4. THE SYNTHESIS OF SUBSTITUTED 1,5-BENZODIAZEPINES. We have synthesized 1,5-benzodiazepines (Scheme I.in App. 1.4). where crotonic acid (1) or methacrilic acid (2) react with 1,2-phenylenediamine (3a) or 4-chloro-1,2-phenylenediamine (3b) leading to tetrahydro-2H-1,5-benzodiazepine-2-ones (4). Condensation of (4) with bromoacetyl chloride followed by 2-diethylaminoethyl-piperidine (6), 4-dimethylaminobutyl-piperidine (7), or diethylaminobutyl-piperidine (8) afforded substituted 1,5-benzodiazepines (9). The reduction in size of the tricycle resulted in a loss of affinity. Cohen, Jin, Reba, J.Heterocyclic Chem. 30, 835-837, 1993; App. 1.4.

5. NOVEL POTENT AND M2-SELECTIVE ANTIMUSCARINIC COMPOUNDS WHICH PENETRATE THE BLOOD BRAIN BARRIER. These compounds (1a-n) were prepared according to the Scheme in App. 1.5. The 4-(methoxyalkyl)phenylacetonitriles were converted to 4-(bromoalkyl)phenylacetic acids (5a-d) by hydrolysis, cleavage, and halogenation. Subsequent reaction of (5a-d) with thionyl chloride, followed by condesation with 11-oxo-10,11-dihydro-5H-dibenzo[b,e][1,4]diazepin (6) yielded the 5-[[4-(haloalkyl)-1-phenyl]acetyl]-10,11-dihydro-5H-dibenzo[b,e][1,4]diazepin-11-ones (7a-d). The reaction of (7a-d) with secondary aliphatic amines provided (1a-n). Further synthetic details are described in the enclosed manuscript. Compounds (1a-n) and three reference compounds (Table V in App. 1.5) were tested for their apparent affinities for the m1 and m2 subtypes. The results demonstrate that (1h) (DIBD) is the most potent compound in the series. DIBD is selective for m2 receptors over m1 receptors by approximately 7-fold. These results also demonstrate that DIBD is approximately 10 times more potent at m2 receptors than is AQ-RA 741. Cohen, Jin, Gitler, de la Cruz, Boulay, Zeeberg, Reba, submitted to Eur. J. Med. Chem.; App. 1.5.

6. FACILE AND GENERAL SYNTHESIS OF 2-, 3-, OR 4-[(DIALKYLAMINO) ALKYL]PYRIDINES AND PIPERIDINES. Reaction of N,N-dialkylaminoalkyl chloride with picolyllithiums (1) provided the pyridine derivative (2) from which the piperidine (3) was synthesized by catalytic hydrogenation. Cohen, Jin, Reba, Liebigs Ann. Chem. pp. 809-810, 1993.

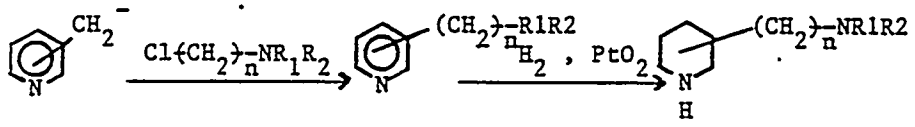

1 2 3

7. SYNTHESIS OF 2- AND 4-IODO-5-[[4-[4-(DIISOBUTYLAMINO)BUTYL]-1-PHENYL]ACETYL]-10,11-DIHYDRO-5H-DIBENZO[b,e] [1,4]DIAZEPIN-11-ONES (10a,b) (SCHEME): 2-IODO-5-[[4-[4-(DIISOBUTYLAMINO)BUTYL]-1-PHENYL]-ACETYL]-10,11-DIHYDRO-5H-DIBENZO[b,e][1,4]DIAZEPIN-11-ONE (2-IDIBD, 10a). It was synthesized according to Scheme. o-Phenylenediamine was condensed with 2-chloro-5-nitrobenzoic acid as described by Giani (1985), to give 2-nitro-11-oxo-10,11-dihydro-5H-dibenzo[b,e][1,4]diazepine (1a). 2-Nitro-11-oxo-10,11-dihydro-5H-dibenzo[b,e]-[1,4]diazepine (1a) was converted into the 2-mino-11-oxo-10,11-dihydro-5H-dibenzo[b,e][1,4]diazepine (2a) by catalytic reduction (palladium on activated carbon). Reaction of (2a) with benzylchloroformate (3) by a modification of Holley (1954) provided 2-benzyloxycarbonyl(Z)amino-11-oxo10,11-dihydro-5H-dibenzo[b,e][1,4]diazepine (4a). The 2-benzyloxycarbonyl(Z)amino-5-[[4-[4-(bromo)butyl]-1-phenyl]acetyl]-10,11-dihydro-5H-dibenzo[b,e][1,4]diazepin-11-one (6a) was prepared by treating (4a) with 4-[4-(bromo)butyl]-phenylacetyl chloride (5). The desired 2-benzyloxycarbonyl(Z)amino-5-[[4-[4-(diisobutylamino)butyl]-1-phenyl]acetyl]-10,11-dihydro-5H-dibenzo[b,e][1,4]diazepin-11-one (8a) was synthesized from reaction of the (6a) with diisobutylamine (7) in acetonitrile by the method described by Cohen (App. 1.5). Compound (8a) was hydrogenated at room temperature in the

presence of palladium on active carbon according to Fletcher (1979) to give the respective amine (**9a**). The 2-iodo-5-[[4-[4-(diisobutylamino)butyl]-1-phenyl]acetyl]10,11-dihydro-5H-dibenzo[b,e][1,4] diazepine-11-one (**10a**) was synthesized from reaction of the diazonium intermediate with potassium iodide by the method described by Cohen (1989). The residue was purified by flash column chromatography (elution with chloroform/methanol 10:1); mp = 137°C. In vitro competition binding studies against [^{3}H]QNB provided the following IC_{50} values. Thus, iodination in the 2-position significantly reduces the binding affinity of DIBD, whereas iodination in the 4-position retain the affinity, but reduces the subtype specificity.

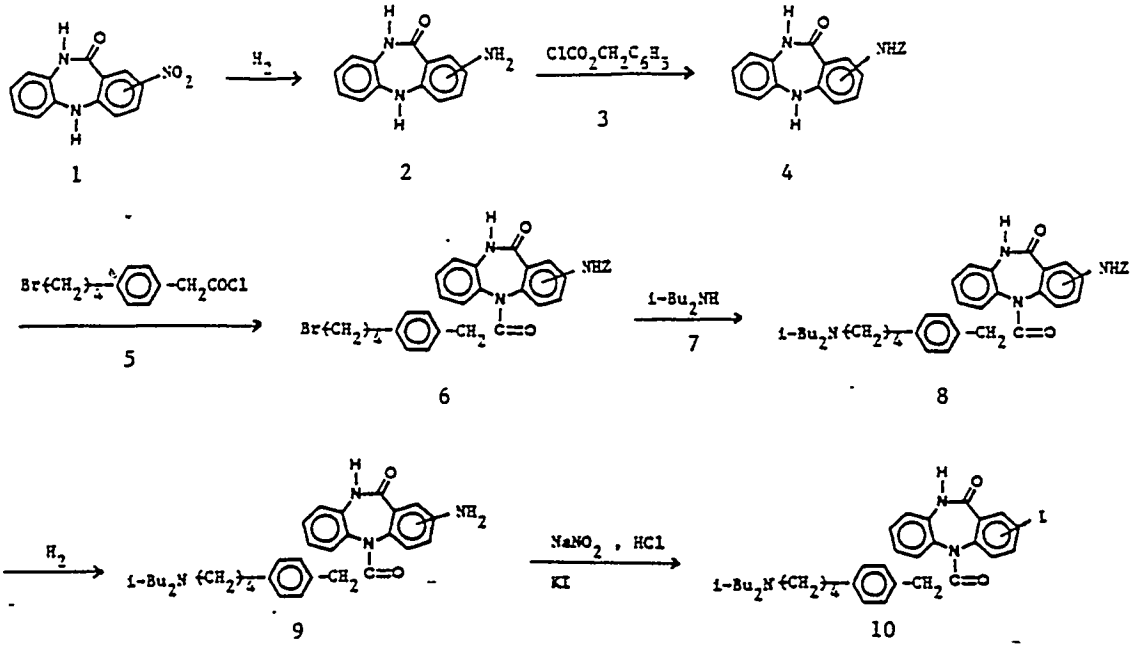

compound	m1	m2	m1/m2
DIBD	25	3.2	7.81
2-IDIBD	200	90	2.22
4-IDIBD	10	5	2.0

8. SYNTHESIS OF 5-[[4-[4-[DI(2-METHYLALLYL)AMINO]BUTYL]-1-PHENYL] ACETYL]-10,11-DIHYDRO-5H-DIBENZO[b,e][1,4]DIAZEPIN-11-ONE [unsaturated precurser for preparing tritiated DIBD (UDIBD)] The best m2-selective antimuscarinic agent studied in the above (section 5) series of compound is 5-[[4-[4-(diisobutylamino)butyl]-1-phenyl]acetyl]-10,11-dihydro-5H-dibenzo[b,e][1,4]diazepin-11-one (DIBD), which penetrates the blood brain barrier and displays in vivo selectivity for the m2-subtype. Since catalytic reduction of a suitable unsaturated precurser with tritium gas is usually the most satisfactory procedure for tritiating a compound, we have prepared the title compound (Scheme). The desired di(2-methylallyl)amine (**3**) was synthesized by treating 2-methylallylamine (**1**) with 2-methylallyl chloride (**2**) in chloroform. Subsequent reaction of amine with 5-[[4-[4-(bromo)butyl]-1-phenyl]acetyl]-10,11-dihydro-5H-dibenzo[b,e][1,4]diazepin-11-one (**4**) in acetonitrile according to Cohen (App. 1.5) yielded the final product (**5**). The pure compound was obtained by flash column chromatogrphy (elution using hexane/ethyl acetate 1:1). Commercially (NEN)-performed tritiation of 61 mg of the unsaturated product UDIBD yielded approximately 5 Ci of crude product.

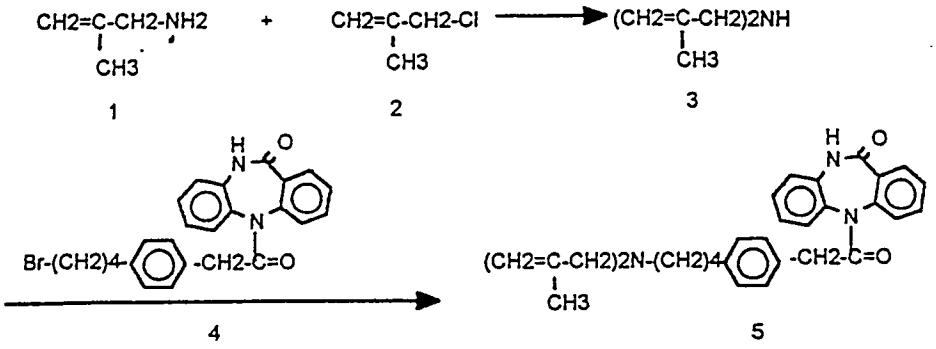

9. SYNTHESIS OF 4-CHLOROALKYLPHENYLACETIC ACIDS AND 4-CHLOROALKYL-CYCLOHEXYLACETIC ACIDS: 4-[4-(CHLORO)BUTYL]PHENYLACETIC ACID AND 4-[4-(CHLORO)BUTYL]CYCLOHEXYLACETIC ACID Chloromethylation of 4-methoxybutylbenzene (1) by dimethoxymethane/HCl took place by heating the mixture at 65°C for 8 h. During this time HCl was bubbled into the reaction mixture to give the corresponding chloromethyl-derivative (2) in the para-position. Reaction of 4-methoxybutylbenzyl chloride (2) with KCN followed by hydrolysis with HCl/HOAc provides 4-[4-(chloro)butyl]phenylacetic acid (3). Catalytic hydrogenation (rhodium on alumina powder) of acetic acid derivatives produces 4-[4-(chloro)butyl]cyclohexylacetic acid (4). Cohen, Jin, Reba, in prep for Synthesis.

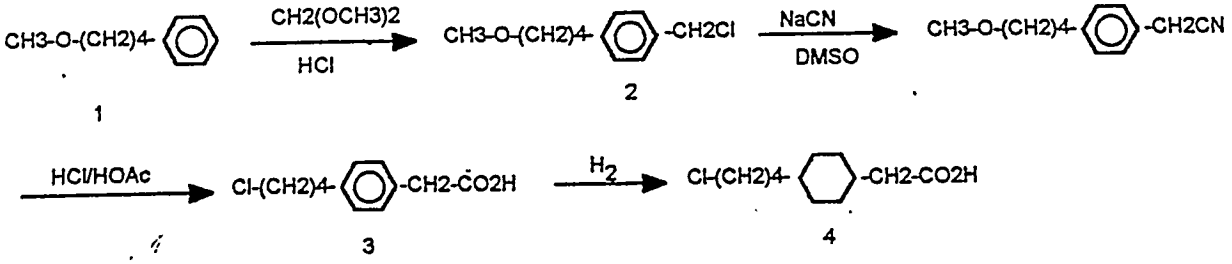

10. SYNTHESIS OF 1- AND 3-FLUORO-5-[[4-[4-(DIALKYLAMINO)BUTYL]-1-PHENYL]ACETYL]-10,11-DIHYDRO-5H-DIBENZO[b,e][1,4]DIAZEPIN-11-ONES (SCHEME): 1-Fluoro-5-[[4-[4-(diisobutylamino)butyl]-1-phenyl]acetyl]-10,11-dihydro-5H-dibenzo[b,e][1,4]diazepin-11-one (6a). 1-F-11-Oxo-10,11-dihydro-5H-dibenzo-[b,e][1,4]diazepine (3a) was prepared by condensation of o-phenylenediamine (1) with 2-chloro-6-fluorobenzoic acid (2) in chlorobenzene by the method reported by Giani (1985). Condensation of (3a) with 4-[4-(bromo)butyl]phenylacetyl chloride (4) provides acyl compound (5a). Subsequent reaction of diisobutylamine with (5a) yields compound (6a).

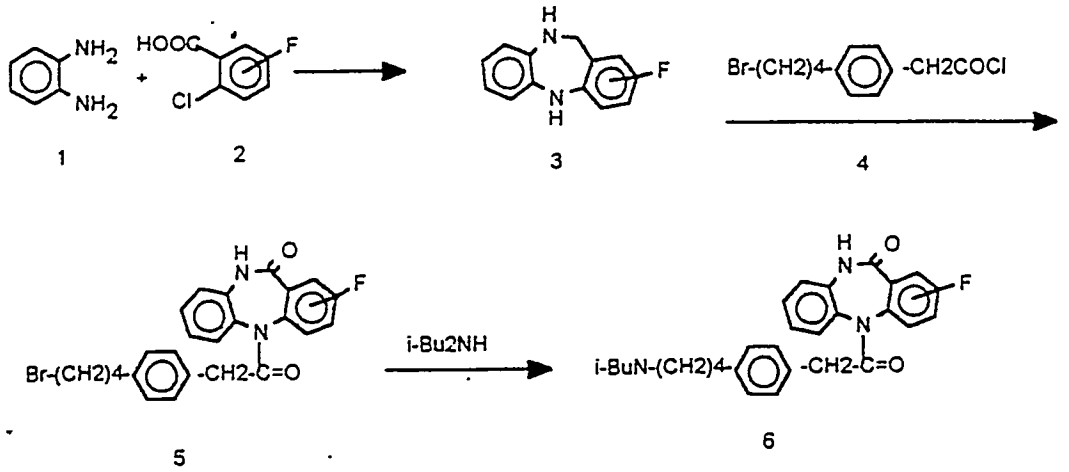

11. SYNTHESIS OF 11-[[4-[(DIALKYLAMINO)BUTYL]-1-PHENYL]ACETYL]-5,11-DIHYDRO-6H-PYRIDO[2,3-b][1,4]BENZODIAZEPIN-6-ONES (SCHEME): 11-[[4-(Diisobutylamino)butyl]-1-phenyl]acetyl]-5,11-dihydro-6H-pyrido[2,3-b][1,4]-benzodiazepin-6-one (6a, R_1 = R_2 = isobutyl; PBID). Condensation of 2-chloro-3-aminopyridine (1) with the methyl anthranilate (2) gives the pyridobenzodiazepinone (3). Reaction of 4-[4-(bromo)butyl]phenylacetyl chloride (4) with pyridobezodiazepinone (3), and then reaction with diisobutylamine provides the final product (6). The pure compounds were obtained by flash column chromatography (elution with 2% NH_4OH for the diethyl, and $CHCl_3$/MeOH 10:1 for the diisobutyl derivative).

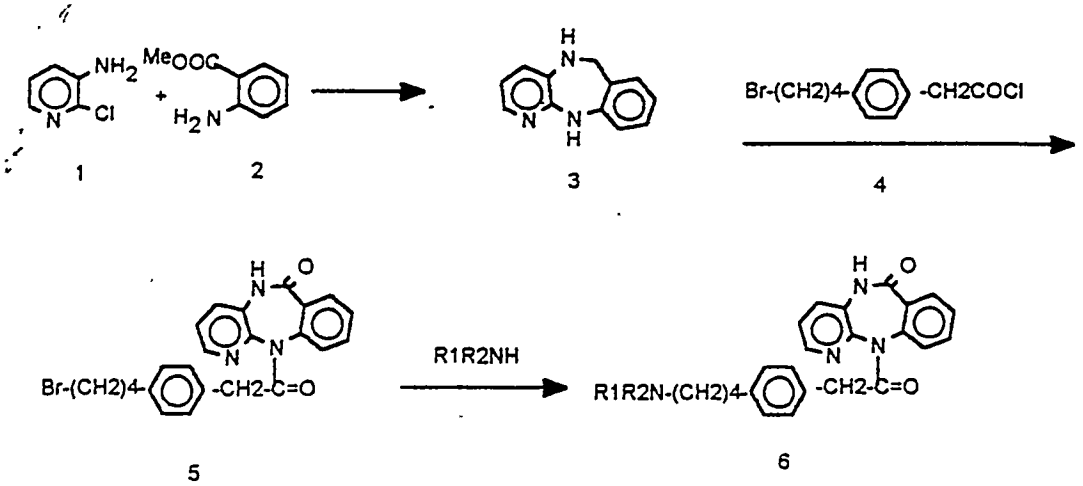

12. SYNTHESIS OF 11-[[4-[3-[ETHYL(2,2-DIMETHYLVALERYL)AMINO]PROPYL]-1-PIPERIDINYL]ACETYL]-5,11-DIHYDRO-6H-PYRIDO[2,3-b][1,4]BENZODIAZEPIN-6-ONE (BIBN 91) AND ITS 8-CHLORO-DERIVATIVE (BIBN 99, 4). The pyrido-benzodiazepinones (3) were prepared by reaction between 2-chloro-3-aminopyridine (1) and methyl 2-aminobenzoate or 2-amino-5-chlorobenzoate (2) (Engel, 1989). Condensation of (3) with chloroacetic acid chloride followed by 4-[3-[ethyl(2,2-dimethylvaleryl)amino]propyl]-1-piperidine gives the final compound (4). The residue was purified by flash column chromatography (elution with hexane/EtAc 1:1 for the BIBN 91, mp 72-75, and 2% NH_4OH in MeOH for BIBN 99, mp 62-65).

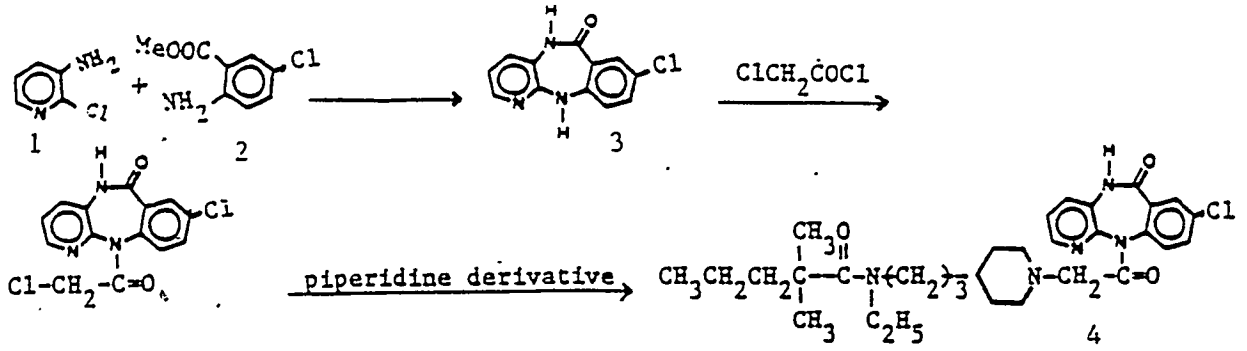

13. SYNTHESIS OF 5-[[4-[3- OR 4-[ETHYL(2,2-DIMETHYLVALERYL)AMINO] PROPYL OR BUTYL]-1-PHENYL]ACETYL]-10,11-DIHYDRO-5h-DIBENZO [b,e] [1,4]DIAZEPIN-11-ONES AND THEIR 2-CHLORO- DERIVATIVES (4). These dibenzodiazepinones are analogues of BIBN 91 and 99, in which the piperidine in the cationic head is replaced by benzene. 11-Oxo-10,11-dihydro-5H-dibenzo[b,e][1,4]diazepine and its chloro- derivatives (1) were prepared according to section 10. Condensation of (1) with 4-[3- or 4-(bromo)propyl or butyl]phenylacetyl chloride (2), provides (3). Reaction of (3) with ethylamine gives (4). Reaction of (4) with 2,2-dimethylvaleryl chloride provides the final compounds (5).

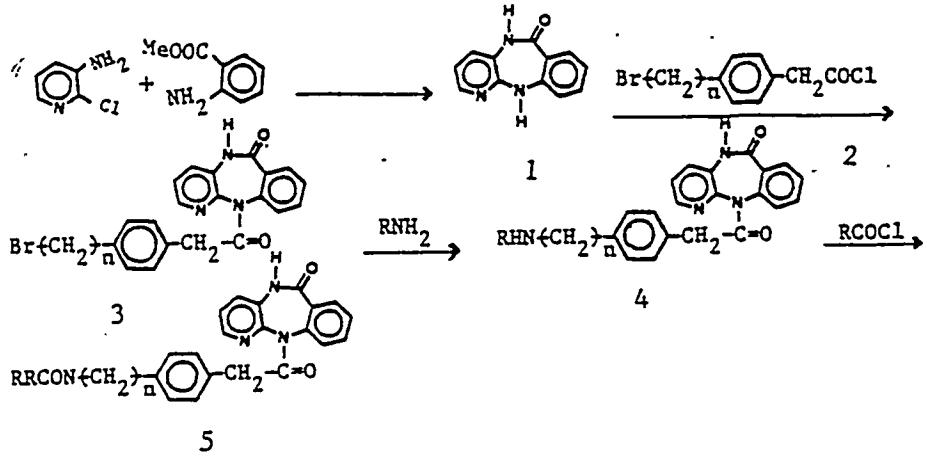

14. SYNTHESIS OF 1-AZABICYCLO[2.2.2]OCT-3-YL-ALPHA-HYDROXY-ALPHA-PHENYL-ALPHA-4-FLUOROPHENYL ACETATE (6). Reaction of 4-fluorobenzophenone (1) with trimethylsilyl cyanide (2) as shown in the Scheme, followed by hydrolysis (3), esterification

(4) with ethanol, and finally transesterification with 3-quinuclidinol (5), yields the 3-quinuclidinyl alpha-(4-fluorophenyl)-alpha-hydroxy-alpha-phenylacetate (6). The crude product was recrystallized from acetone, mp 134-137.

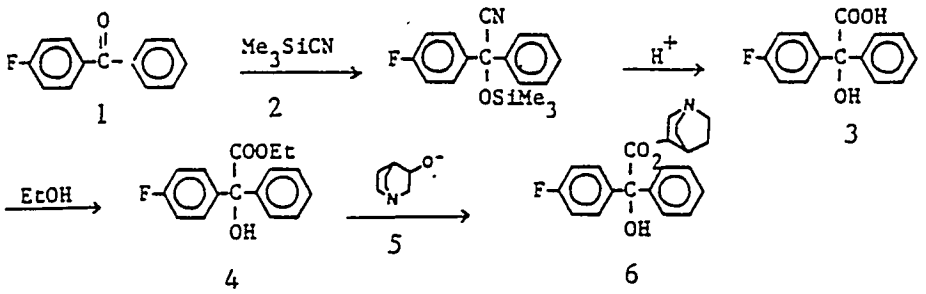

PHARMACOLOGY

1. A NOVEL MUSCARINIC RECEPTOR LIGAND WHICH PENETRATES THE BLOOD BRAIN BARRIER AND DISPLAYS IN VIVO SELECTIVITY FOR THE m2 SUBTYPE. We have used competition studies against currently existing muscarinic receptor radioligands to infer the in vitro and in vivo properties of a novel muscarinic receptor ligand, 5-[[4-[4-(diisobutylamino)butyl]-1-phenyl]acetyl]-10,11-dihydro-5H-dibenzo[b,e][1,4]-diazepin-11-one (DIBD). In vitro competition studies against [^{3}H](R)-3-quinuclidinylbenzilate ([^{3}H]QNB) and [^{3}H]N-methylscopolamine ([^{3}H]NMS), using membranes derived from transfected cells expressing only m1, m2, m3, or m4 receptor subtypes, indicate that DIBD is selective for m2/m4 over m1/m3. In vivo competition studies against (R,R)-[^{125}I]IQNB indicates that DIBD crosses the blood brain barrier (BBB). The relationship of the regional percentage decrease in (R,R)-[^{125}I]IQNB versus the percentage of each of the receptor subtypes indicates that DIBD competes more effectively in those brain regions which are known to be enriched in the m2, relative to the m1, m3, and m4, receptor subtype; however, analysis of the data using a mathematical model shows that caution is required when interpreting the in vivo results. We conclude that a radiolabeled derivative of DIBD may be of use in tomographic study of the loss of m2 in AD. Gitler, Cohen, De La Cruz, Boulay, Jin, Zeeberg, Reba., Life Sci. 53, 1743 (1993); App. 1.6.

2. [^{3}H]QNB DISPLAYS IN VIVO SELECTIVITY FOR THE m2 SUBTYPE. We report here the results of in vivo studies, using both carrier-free and low specific activity [^{3}H]QNB, which show that [^{3}H]QNB exhibits a substantial in vivo m2-selectivity. We conclude that a radiolabeled derivative of QNB, possibly labeled with ^{18}F, may be of use in positron emission tomographic (PET) study of the loss of m2 receptors in AD. Gitler, De La Cruz, Zeeberg, Reba. Submitted to Life Sci. (1994); App. 1.7.

3. USE OF EX VIVO BINDING TO MEASURE THE BRAIN CONCENTRATIONS OF PUTATIVE RADIOLIGANDS. We describe an ex vivo binding technique for measuring the brain concentration of injected unlabeled compounds. The pharmacokinetics of brain penetration of three muscarinic antagonists are described: QNB, BrQNB and the 2-thienyl derivative of Br-QNB and were found to compare favorably to previous studies using [3H]QNB. These studies demonstrate the effectiveness of ex vivo binding in assessing the brain concentration of peripherally administered unlabeled compounds. Baumgold, Ling, Reba Nucl Med Biol, Int J Radiat Appl Instrum Part B, 19, 513 (1992).

4. A NOVEL M2-SELECTIVE MUSCARINIC ANTAGONIST: BINDING CHARACTERISTICS AND AUTORADIOGRAPHIC DISTRIBUTION IN RAT BRAIN. A bio-isoster of AQ-RA 741 is both one order of magnitude more potent and slightly more selective than previously described compounds. DIBA, a di-benz- derivative of AQ-RA 741, in which the pyridine of the tricycle is replaced with a benzene ring, had K_i values of 4, 0.3, 11 and 2 nM at m1 through m4 receptors, respectively. These

values were determined in competition studies with [^{3}H]-N-methylscopolamine ([^{3}H]NMS) in membranes from transfected A9 L cells (m1 and m3), rat heart (m2) and NG108-15 cells (m4). AQ-RA 741 had K_i values of 34, 4, 86 and 15 nM at each of these receptors. The autoradiographic distribution of DIBA binding sites was determined by displacement of [^{3}H]NMS in rat brain. At low concentration, DIBA displaced [^{3}H]NMS most significantly from superior colliculi, thalamus, hypothalamus, pontine nucleus, and interpeduncular nucleus, and not appreciably from caudate nucleus, cerebral cortical regions, or hippocampus, consistent with its binding to m2 receptors. These data indicate that DIBA is the most potent, m2-selective muscarinic antagonist yet described. Gitler, Reba, Cohen, Rzeszotarski, Baumgold Brain Res., vol. 582, pp.253-260, 1992.

5. BINDING OF RADIOIODINATED SPECT LIGANDS TO TRANSFECTED CELL MEMBRANES EXPRESSING SINGLE MUSCARINIC RECEPTOR SUBTYPES. The equilibrium dissociation constant and the kinetic rate constants were determined for the binding of (R)-[^{3}H]3-quinuclidinyl benzilate ([^{3}H]QNB) and [^{125}I]3-quinuclidinyl-4-iodobenzilate ((R,R)- and (R,S)-[^{125}I]IQNB) to transfected cell membranes expressing one single muscarinic acetylcholine receptor (mAChR) subtype. The association and dissociation kinetics for the m2 subtype were more rapid than for the m1 and m3 subtypes. The differential kinetic properties may be useful for the single photon emission computed tomographic (SPECT) evaluation of regional mAChR subtype alterations in disease states. Zeeberg, Gitler, Baumgold, de la Cruz, and Reba. BBRC 179, 768-775, 1991.

6. KINETIC ANALYSIS OF RAT PAROTID GLAND MUSCARINIC RECEPTORS IN VIVO: COMPARISON WITH BRAIN AND HEART. Short-term infusion studies in vivo showed that the "instantaneous" reversible binding of (RR)- and (SS)-IQNB was high in the parotid (greater nonspecific binding potential), intermediate in the heart, and lowest in cortex and cerebellum. Long-term bolus injection studies showed that the parotid gland mAChRs possessed a binding potential for receptor specific sites (380), which was intermediate between that of parietal cortex (930) and cerebellum (10) and greater than that of heart (165). In vitro binding to plasma membranes was consistent with the in vivo findings. Thus mAChRs can be evaluated in vivo in a nonexcitable tissue with the use of stereospecific ligands and a pharmacokinetic approach. The data suggest that IQNB, a mAChR antagonist, can identify characteristics of specific binding sites, which may reflect tissue differences. Hiramatsu, Kawai, Reba, Simon, Baum, and Blasberg. Am. J. Physiol. 264, G541-552, 1993.

7. IN VIVO DISSOCIATION KINETICS OF [^{3}H]QUINUCLIDINYL BENZILATE: RELATIONSHIP TO MUSCARINIC RECEPTOR CONCENTRATION AND IN VITRO KINETICS. The in vivo washout kinetics of [^{3}H]quinuclidinyl benzilate ([^{3}H]QNB) varies significantly in various structures in the rat brain. The slowest washout rates are from the hippocampus, corpus striatum, and cortex, intermediate rates are exhibited from the thalamus and colliculi, while the fastest washout rate is from the cerebellum. We have also demonstrated a difference in the in vitro dissociation rates (k_{-1}) of [^{3}H]QNB from various structures. The k_{-1} for the hippocampus, corpus striatum, and cortex is two-fold slower than that observed in the thalamus, colliculi, and cerebellum. The differences in the in vitro dissociation kinetics are not, however, sufficient to explain the differences in the in vivo washout kinetics. We have developed a theoretical formulation which describes conditions under which the washout kinetics are a function of the concentration of receptor in a structure. Furthermaore, we present a graphical method in which a plot of the reciprocal of the observed washout rate constant, $1/k_{(obs)}$ vs receptor concentration is linear. Analysis of the washout kinetics of [^{3}H]QNB from varius structures of the CNS of rat were well described by this theory when the differences in in vitro k_{-1} are included. Gibson, Zeeberg, Melograna, Wang, Ruch, Braun, and Reba. Brain Res. 553, 110-116, 1991.

8. IN VIVO NONSPECIFIC BINDING PARAMETERS OF (R,R)-[^{125}I]4IQNB ESTIMATED FROM THE PHARMACOKINETICS OF THE (S,S)-[^{125}I]4IQNB STEREOISOMER (LETTER). A proposed method of determining nonspecific binding parameters for a radioligand is to measure the pharmacokinetics of a stereoisomer whose affinity for receptor is lower. We have investigated a specific example to gain a better understanding of when the parameters derived from the stereoisomer may be used to estimate the the nonspecific binding of the original radioligand. Our analysis of data

from a recent report suggests that even a stereoisomer with a low relative affinity can exhibit a high degree of specific binding. Hertzman and Zeeberg. J. Cereb. Blood Flow Metab. 12, 173-176, 1992.

9. CONCERNING THE DISTRIBUTION OF CEREBRAL MUSCARINIC ACETYLCHOLINE RECEPTORS IN ALZHEIMER'S DISEASE (LETTER). An article describing the distribution of mAChR in vivo in patients with Alzheimer's disease (AD) using SPECT imaging of the distribution of [^{123}I]IQNB finds that there is " . . . a significant reduction bilaterally in the posterior temporal cortex of the patients with Alzheimer's disease compared with controls . . . " The authors conclude " . . . It is likely that the images reflect the distribution of the relative density of a subpopulation of muscarinic receptors. The majority of patients with primary degenerative dementia had qualitatively abnormal IQNB SPECT scans, perhaps because of focal areas of reduced receptor density . . ." However, although it is possible that the IQNB localization deficits reflect a mAChR deficit, we show that the arguments presented do not distinguish this possibility from the possibility that the deficits reflect the known blood flow deficit. Zeeberg. Arch. Neurol. 48, 1117-1118, 1991.

10. IN VIVO PHARMACOKINETIC SENSITIVITY OF (R,R)-[^{125}I]IQNB ACCUMULATION AS A REFLECTION OF THE CONCENTRATIONS OF MUSCARINIC ACETYLCHOLINE RECEPTOR SUBTYPES IN RAT BRAIN. To test the hypothesis that a single human brain SPECT image of (R,R)-[^{123}I]3-quinuclidinyl-4-iodobenzilate ([^{123}I]IQNB) can be used to estimate the concentrations of regional muscarinic acetylcholine receptor (mAChR) subtypes, we applied an experimental approach to determine the degree of sensitivity with which [^{125}I]IQNB accumulation reflects mAChR subtype concentrations in the rat brain. This approach involves measuring the effect of partial mAChR blockade upon [^{125}I]IQNB accumulation within a given brain region. Partial mAChR blockade was effected by preinjecting QNB. In each region studied, the experimentally determined sensitivity at the naturally-occurring mAChR concentration was between 1 to 2. Because of this variation in sensitivity between regions, neither the absolute amounts of radioactivity nor the relative changes in radioactivity in two different brain regions can be directly compared and interpreted as reflecting the underlying regional mAChR concentration. This complicated behavior is in part a result of the different proportions of m1, m2, m3, and m4 subtypes in different brain regions. Even if the underlying pharmacokinetic properties are very similar for two brain regions, neither the absolute amounts of radioactivity nor the relative changes in radioactivity in the two regions can be compared and interpreted as reflecting the underlying regional mAChR concentration, since the pharmacokinetic sensitivity reflecting changes in one mAChR subtype may differ from the pharmacokinetic sensitivity reflecting changes in another mAChR subtype. Gitler, Zeeberg, Reba, de la Cruz, John, Cohen. Submitted to Life. Sci.

11. MUSCARINIC RECEPTOR SELECTIVITIES OF 3-QUINUCLIDINYL 8-XANTHENECARBOXYLATE (QNX) IN RAT BRAIN. We have determined the binding of (R)-3-Quinuclidinyl 8-xanthenecarboxylate to muscarinic acetylcholine receptor preparations from rat cortex, hippocampus, caudate/putamen, thalamus, pons and colliculate bodies. The competition curves against [^{3}H]quinuclidinyl benzilate are well described by a two site model with a difference in affinity between the two sites of 12-fold. The proportions of high affinity site vary from 100% in the caudate/putamen to 0% in the pons/medulla. The selectivities are different from those measured by pirenzepine and are consistent with QNX exhibiting similar affinity for the M_1, M_3, and M_4 receptors with lower affinity for the M_2 receptor. This assignment was confirmed by determining the affinities of QNX using cloned subtypes. Gibson, Schneidau, Gitler, Baumgold, Zeeberg, Reba. Life Sci, 54, 1757, 1994.

12. SPECIFIC BINDING COMPONENT OF THE "INACTIVE" STEREOISOMER (S,S)-[^{125}I]IQNB TO RAT BRAIN MUSCARINIC RECEPTORS IN VIVO. One technique for measuring in vivo specific and nonspecific binding involves using both active and inactive stereoisomers of a radioligand for a receptor. However, the inactive isomer may have sufficient affinity that its uptake partially reflects specific binding. This phenomenon has been previously predicted on a theoretical basis using pharmacokinetic modeling for (S,S)-[^{125}I]IQNB, the inactive isomer of the mAChR radioligand (R,R)-[^{125}I]IQNB. We have applied a second technique for measuring in vivo nonspecific binding, which involves studying the inhibition induced by preinjection of a large excess of a competing nonradioactive ligand. Our application of this technique differed from the usual application, since it was

15. IN VIVO RESULTS WITH PBID AND IQNP. In vivo studies of the regional blockade of [^{125}I]IQNB retention induced by the nonradioactive competitors PBID (m2-selective antagonist; 10) and IQNP (m1-selective antagonist; see section 14 above) were carried out in rat brain, followed by dissection of brain regions. In order to correct for nonspecific binding and to reduce the variance between individual animals, for each rat, its own cerebellum value was first subtracted from each brain region, followed by normalization effected by dividing each brain region by the average of the m1-rich regions (that is csr, csl, fcr, fcl, hippo) in that brain. Thus, changes will be measured relative to the average change in the m1-rich regions. For the special case of a strongly m2-selective antagonist, the change in the m1-rich regions will be close to zero, so that the changes can then be interpreted as absolute rather than relative. PBID causes a substantial decrease in the m2-rich regions, (sc, ic, pons, med), thus demonstrating its effective in vivo m2-selectivity. In contrast, the m1-selective IQNP causes increases in the m2-rich regions. Thus, IQNP is a negative control validating the PBID result.

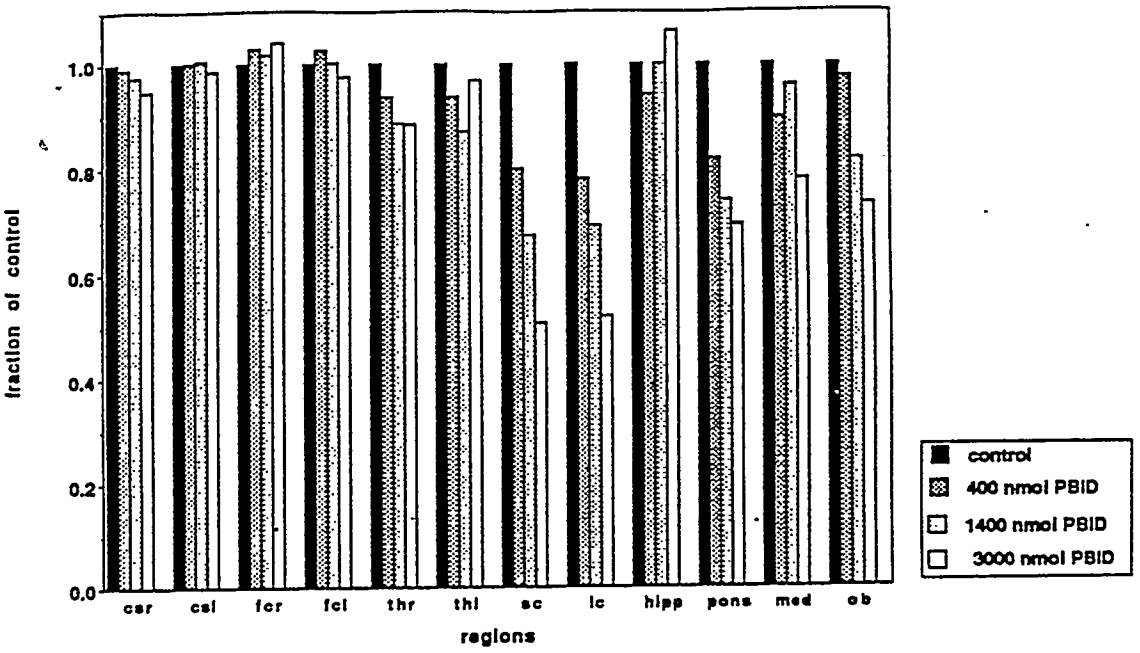

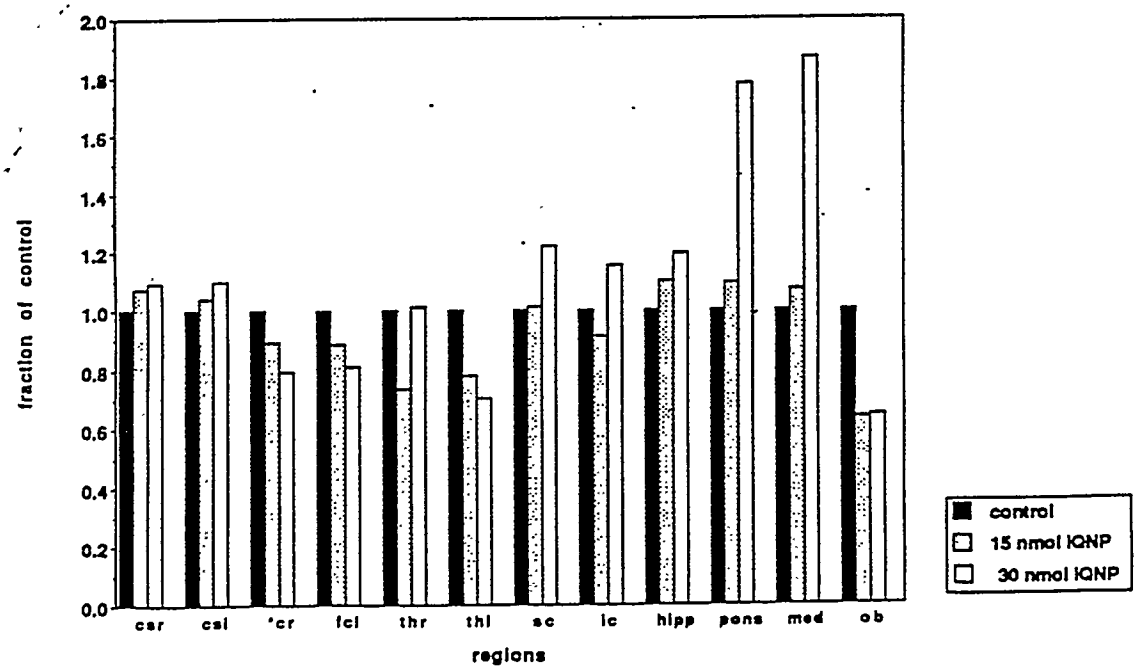

used to study the uptake of the inactive isomer ((S,S)-[^{125}I]IQNB), rather than the active isomer. The results of the competition studies indicate that there is substantial specific binding for (S,S)-[^{125}I]IQNB. Boulay, McRee, Cohen, Sood, Zeeberg, Reba. App. 1.9; Submitted to Life Sci.

13. GRAPHICAL ANALYSIS OF FLUOROALKYL QNB DEMONSTRATING IN VIVO m2 mAChR SELECTIVITY. Recent in vivo studies using [^{3}H]QNB by itself or QNB in competition with [^{125}I]IQNB demonstrate an in vivo m2-selectivity for QNB. IQNB, on the other hand, does not appear to exhibit significant in vivo m2-selectivity. We demonstrate here by in vivo competition with [^{125}I]IQNB that a series of (R)-quinuclidinyl-(S)-(4-fluoroalkyl)benzilates retains the m2-selectivity of QNB. The results for a 50 nmol coinjection of FMeQNB typify those for FEt- and FPrQNB. The only positive correlation is with the m2 subtype. Thus a suitably radiofluorinated derivative of QNB may be useful for quantification of the loss of the m2 mAChR subtype in AD. Zeeberg, Kieswetter, Lee, Paik, Park, Reba, Eckelman. Submitted to SNM 94; in prep for Life Sci.

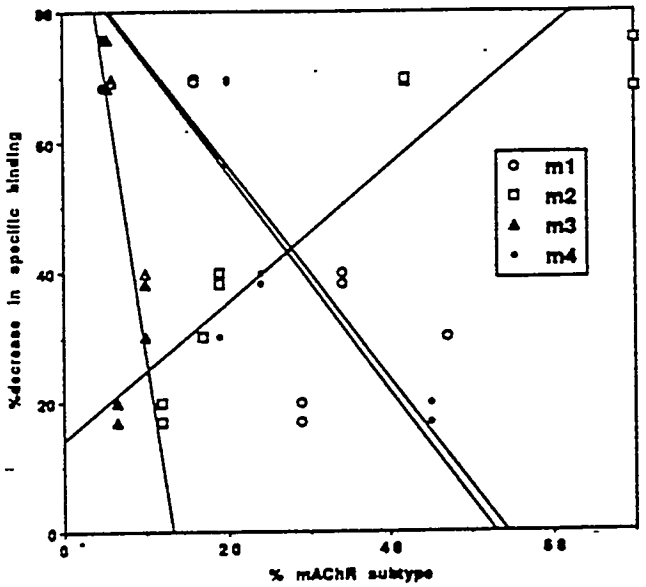

Coinjection of 50 nmol FMeQNB and nca [^{125}I]IQNB. Plotted according to Gitler et al (Life Sci, 53, 1743, 1993).

14. EFFECTS OF ABSOLUTE CONFIGURATION OF IQNP ON MUSCARINIC RECEPTOR SUBTYPE SELECTIVITY IN VITRO AND IN VIVO. IQNP (1-azabicyclo[2.2.2]oct-3yl α-hydroxy-α-(1-iodo-1-propen-3-yl)-α-phenylacetate), a high affinity muscarinic ligand with high cerebral uptake and long retention, contains two chiral centers in addition to vinyl iodide stereochemistry. In vitro studies show that E-(R,R)-IQNP is 100 times more selective for m1 than m2 subtype as compared to E-(R,S), which was confirmed by in vivo results. In contrast, in vivo, Z-(R,R) has high uptake in m2 rich tissues (heart and cerebellum). Blocking studies with subtype-selective ligands confirm these data which illustrate the importance of molecular configuration on receptor subtype selectivity. These studies show that these isomers of IQNP are good candidates for future studies of receptor subtypes. McPherson, Lambert, Zeeberg, Sood, McRee, Reba, and Knapp. Submitted to SNM 94.

	In Vitro (nM)			In Vivo, Mean % ID/G (t=6h)		
IQNP	m1	m2	m4	Striatum	Cerebellum	Heart
E-(R,R)	0.383	29.6	0.356	1.38	0.04	0.10
E-(R,S)	6.83	41.2	2.39	0.04	0.01	0.06
Z-(R,R)	-	-	-	1,52	0.28	0.70
Z-(R,S)	-	-	-	1.15	0.10	0.34

16. PRELIMINARY AUTORADIOGRAPHIC RESULTS CHARACTERIZING [^{125}I]IQNB BINDING TO THE ANTERO-VENTRAL (AV) NUCLEUS. 10 u thick coronal rat brain slices through the AV nucleus were incubated in 0.6 nM nca [^{125}I]IQNB (SA approximately 400 Ci/mmol) in TRIS buffer at ambient temperature for 4 h in the presence or absence of 10 uM atropine. The slices were apposed to x-ray film for 24 h and quantified using a computerized image-analysis system RAS-3000 (Loats, Amersham). The preliminary results (see photographs in App. 1.10) indicate our ability to perform quantitative autoradiographic analysis of the effects of various forms of pharmacological treatment upon the binding of radioligands to the AV nucleus. This forms the basis for our proposed in vivo studies exploiting the high m2 subtype concentration in the AV nucleus (Mash, 1986; Gibson, 1989, 1992).

17. IN VITRO AND IN VIVO RESULTS WITH α-CHLOROIMPERIALINE. In vitro competition studies against [^{3}H]NMS using transfected cell membranes resulted in the following IC_{50} values (in nM) for α-chloroimperialine: m1 7.6; m2 0.70; m3 44.0; m4 4.7. A single in vivo competition study (1000 nmol α-chloroimperialine injected/rat) against [^{125}I]IQNB indicated substantial blocking (about 30-50%) of [^{125}I]IQNB binding in all brain regions except cerebellum. There was no indication of in vivo subtype selectivity, but the experiment would need to be repeated under a variety of conditions (incubation times, coinjection versus preinjection, etc) to draw a firm conclusion on this point. Because of the extreme expense of the commercially available starting materials ($75 to $100 per mg), and the difficult chemistry required in order to develop a labeled compound suitable for SPECT or PET imaging, we will not pursue the chemistry of the imperialine derivatives in this proposal.

18. SUBTYPE SELECTIVITIES OF NOVEL PYRIDOBENZODIAZEPINONE AND DIBENZODIAZEPINONE DERIVATIVES.

Table 1

			Kd(nM)			
Compound	X	n	m1	m2	m4	m1/m2
4a(BIBN 91)	H	3	6.63E+02	1.07E+01	3.62E+01	61.96
4b(BIBN 99)	Cl	3	5.51E+03	4.42E+01	2.13E+02	124.69
12a	H	3	1.00E+04	3.71E+03	ND	2.70
12b	H	4	1.00E+04	1.06E+03	ND	9.39
12c	Cl	3	1.00E+04	5.94E+03	ND	1.68
12d	Cl	4	5.00E+03	2.65E+03	ND	1.89

Table 2

				Kd(nM)			
Compound	X	Y	R	m1	m2	m4	m1/m2
10a	N	CH	C_2H_5	2.02E+02	9.60E+00	ND	20.99
10b	N	CH	$i\text{-}C_4H_9$	2.73E+01	1.28E+00	4.36E	21.34

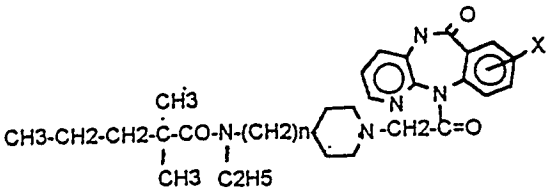

4

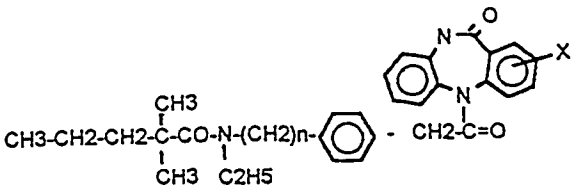

12

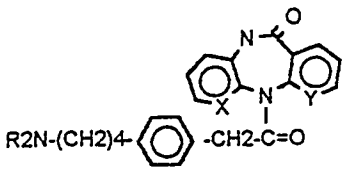

10

IMAGING PHYSICS

1. 3D SPECT SIMULATIONS OF A COMPLEX 3D MATHEMATICAL BRAIN MODEL: EFFECTS OF DETECTOR RESPONSE, ATTENUATION, SCATTER, AND STATISTICAL NOISE. The imaging characteristics of parallel hole SPECT, including attenuation, scatter, and noise, were investigated by simulations based on a 3D brain model of grey and white matter isotope distributions. The results demonstrate significant artifacts in reconstructed human brain images. In the absence of attenuation, scatter, and noise, the reconstructed values along a cortical circumferential profile in a transverse slice through the basal ganglia varied by a factor of 2.40, although the original values were identical in all cortical regions. This variation causes inaccuracies in regional radioactivity quantification. Inclusion of attenuation, scatter, and noise in the simulation caused additional artifacts, and resulted in reconstructed images which corresponded closely to reconstructed images of the actual 3D brain phantom constructed from the same set of data as the mathematical 3D brain model. The major degrading factor in SPECT neuroimaging is the detector response function. The other sources of degradations are either of smaller magnitude (scatter, noise) or can be corrected with sufficient accuracy (attenuation). Kim, Zeeberg, Fahey, Hoffman, Reba. IEEE Trans. Med. Imag., vol. 11, pp. 176-184, 1992.

2. COMPENSATION FOR 3-D DETECTOR RESPONSE, ATTENUATION, AND SCATTER IN SPECT GREY MATTER IMAGING USING AN ITERATIVE RECONSTRUCTION ALGORITHM WHICH INCORPORATES A HIGH RESOLUTION ANATOMICAL IMAGE. The reconstructed values depend upon the shape and size of the brain region as strongly as upon the true radioactivity concentration. We report here the results of applying an iterative reconstruction algorithm (IRA) to compensate for the shape- and size dependence, as well as for attenuation and scatter. The IRA incorporates an accurate three-dimensional (3-D) model of the detector response (3-DPSF) and utilizes a magnetic resonance image (MRI) to define the anatomical features of the brain being imaged by segmenting the grey, white, and ventricular regions. The IRA was validated by simulation studies which utilized a slice through the basal ganglia in the realistic Hoffman 3-D mathematical brain model. Visual inspection, circumferential cortical profiles, and histograms and scatter plots of the global error distributions indicate that FBP images deviate significantly from the true radioactivity distribution, whereas IRA images are nearly identical to the true radioactivity distribution, except for random fluctuations due to statistical noise. Kim, Zeeberg, Reba. J. Nucl. Med. vol. 33, pp. 1225-1234, 1992.

3. EVALUATION OF RECONSTRUCTION ALGORITHMS IN SPECT NEUROIMAGING: I. COMPARISON OF STATISTICAL NOISE IN SPECT NEUROIMAGES WITH "NAIVE" AND "REALISTIC" PREDICTIONS. It is normally expected that an algorithm which improves spatial resolution and quantitative accuracy might also increase the magnitude of the statistical noise in the reconstructed image. However, the noise properties in the IRA images are very similar to those in the FBP images. In fact, the noise magnitude in both the FBP and IRA images is just slightly greater than

that computed by the "naive prediction," which presumably is a lower limit to the amount of statistical noise in a reconstructed image. Kim, Zeeberg, Reba Phys. Med. Biol. 38, 863 (1993a).

4. EVALUATION OF RECONSTRUCTION ALGORITHMS IN SPECT NEUROIMAGING: II. COMPUTATION OF DETERMINISTIC AND STATISTICAL ERROR COMPONENTS. For the reconstruction of a series of computer simulations of statistically-independent noisy realizations of projection data, the *total error* for the i^{th} reconstructed voxel in the r^{th} realization, $E_{r,i}$, is composed of the *statistical error*, $S_{r,i}$, and the (deterministic) *inaccuracy in the presence of noise*, D_i^+. D_i^+ is composed of the (deterministic) *inaccuracy in the absence of noise*, D_i^-, and the (deterministic) *additional inaccuracy in the presence of noise*, D_i^Δ. $E\{E_{r,i}\}$, the theoretical expected value of $E_{r,i}$, is given by $E\{E_{r,i}\} = E\{D_i^+\} + E\{S_{r,i}\}$. Similarly, $E\{D_i^+\} = E\{D_i^-\} + E\{D_i^\Delta\}$. The corresponding theoretical variances are given by $\sigma^2(E_{r,i}) = \sigma^2(D_i^+) + 2C(D_i^+, S_{r,i}) + \sigma^2(S_{r,i})$ and $\sigma^2(D_i^+) = \sigma^2(D_i^-) + 2C(D_i^-, D_i^\Delta) + \sigma^2(D_i^\Delta)$, where $C(.,.)$ is the covariance. We used these relationships to evaluate 3 reconstruction algorithms: filtered back projection (FBP), an iterative reconstruction algorithm (IRA), and a version of the IRA incorporating a linear transformation (TIRA). For simulated brain images with projection data degraded by convolution of the true radioactivity distribution with a distance-dependent detector response function, for FBP the major contribution to both $E\{E_{r,i}\}$ and $\sigma^2(E_{r,i})$ was D_i^-. For IRA and TIRA, the major contributions to $E\{E_{r,i}\}$ were D_i^- and D_i^Δ, and the major contribution to $\sigma^2(E_{r,i})$ was $S_{r,i}$, although in some cases D_i^Δ also was a contributing factor. Furthermore, the errors due to $\sigma^2(E_{r,i})$ {that is, $[\sigma^2(E_{r,i})]^{.5}$} were more severe than those due to $E\{E_{r,i}\}$. Unlike FBP, the effects of statistical noise are an important limiting factor for the IRA and TIRA. Kim, Zeeberg, Reba Phys. Med. Biol. 38, 881 (1993b).

5. GREY AND WHITE MATTER SPECT NEUROIMAGE RECONSTRUCTION: ITERATIVE RECONSTRUCTION USING A HIGH RESOLUTION ANATOMICAL IMAGE TO CORRECT FOR 3-D DETECTOR RESPONSE, ATTENUATION, AND SCATTER. In the presence of a 3D distance-dependent detector response, attenuation, scatter, and statistical noise, an iterative reconstruction algorithm (IRA) for the quantitative reconstruction of SPECT brain images overcomes major limitations of filtered back projection (FBP): (a) the nonuniformity within the grey (or white) matter voxels which results even though the true model is uniform within these voxels; (b) a significantly lower ratio of grey/white matter voxel values than in the true model; and (c) an inability to detect an altered radioactivity value within the grey (or white) matter voxels. The IRA permits the detection of subtle variations in both grey and white matter radioactivity, as demonstrated for both sinusoidal and deficit brain models. IRA performs partial voluming, attenuation, and scatter corrections. Statistical noise is a limiting factor. Kim, Zeeberg, Reba, 1992 IEEE NSS Conf Rec, vol. 2, pp. 1002-1004, 1993.

KINETIC MODELING

1. PHARMACOKINETIC SIMULATIONS OF SPECT QUANTITATION OF THE M2 MUSCARINIC NEURORECEPTOR SUBTYPE IN DISEASE STATES USING RADIOIODINATED (R,R)-4IQNB. Emission tomgraphic study of the loss of M2 receptors in AD is limited by the fact that there is currently no available M2-selective radioligand which can penetrate the blood-brain barrier. However, by taking advantage of the different pharmacokinetic properties of (R,R)-[^{123}I]IQNB, it may be possible to estimate losses in M2. We hypothesize that the difference between an early study and a late study should provide information on the M2-receptor population. In order to test this hypothesis, we present here the results of pharmacokinetic simulations of the in vivo localization of (R,R)-[^{123}I]IQNB in brain regions containing various proportions of M1 and M2 subtypes. These results permit us to conclude that SPECT imaging of (R,R)-[^{123}I]IQNB localization can potentially be used to quantitate changes in the M2 subtype in a disease state within a brain region for which the ratio M2/M1 is sufficiently high in normal individuals. Zeeberg, Kim, Reba. Life Sci., vol. 51, pp. 661-670, 1992.

2. ESTIMATION OF RELATIVE REGIONAL NEURORECEPTOR CONCENTRATION BY EMISSION COMPUTED TOMOGRAPHY: THEORETICAL COMPARISONS OF USING A SINGLE

LATE IMAGE OR A LATE PLUS EARLY IMAGE. We have applied a computer simulations to determine the effect, upon the accuracy and precision of the estimated ratio of ipsilateral and contralateral receptor concentrations, of (1) the values of the sensitivities to receptor and delivery, (2) the selection of a particular operational procedure for interpreting the ipsilateral and contralateral radioactivity localizations, and (3) the inclusion of radioactivity localizations at an early time point in addition to the later time point. We have found that the accuracy and precision depend upon the sensitivities for both delivery and receptor, and that the effects of these two sensitivities can oppose each other or can result in a coordinated effect. Incorporation of data at an early time point results in a significant improvement in both the accuracy and precision. There is an insignificant effect of subtraction of the radioactivity localization in a control region. Zeeberg, Kim, Reba. IEEE Trans. Med. Imag. 12, 497 (1993).

LIST OF PUBLICATIONS

CHEMISTRY

1. SYNTHESIS AND RECEPTOR AFFINITIES OF NEW 3-QUINUCLIDINYL ALPHA-HETEROARYL-ALPHA-ARYL-ALPHA-HYDROXYACETATES. Victor I. Cohen, Raymond E. Gibson, Linda H. Fan, Rosanna De La Cruz, Miriam S. Gitler, Erin Hariman, and Richard C. Reba J.Pharm.Sci., 81, 326-329, 1992.

2. SYNTHESIS AND STRUCTURE-ACTIVITY RELATIONSHIP OF SOME 5-[[[(DIALKYLAMINO)ALKYL]-1-PIPERIDINYL]ACETYL]-10,11-DIHYDRO-5H-DIBENZO[b,e][1,4]DIAZEPIN-11-ONES. Cohen et al. J.Med.Chem. 36,162-165, 1993.

3. SYNTHESIS OF SOME DIBENZODIAZEPINONES AS POTENT m2-SELECTIVE ANTIMUSCARINIC COMPOUNDS. Cohen et al. J Heterocyclic Chem, in press.

4. THE SYNTHESIS OF SUBSTITUTED 1,5-BENZODIAZEPINES. Cohen et al., J. Heterocyclic Chem., 30, 835-837, 1993.

5. NOVEL, POTENT AND M2-SELECTIVE ANTIMUSCARINIC COMPOUNDS WHICH PENETRATE THE BLOOD BRAIN BARRIER. Cohen et al., submitted to Eur. J. Med. Chem.

6. SYNTHESIS OF 5-[[4-[4-[DI(2-METHYLALLYL)AMINO]BUTYL]-1-PHENYL]ACETYL]-10,11-DIHYDRO-5H-DIBENZO[B,E][1,4]DIAZEPIN-11-ONE. Cohen et al., In preparation for Liebigs Ann. Chem.

7. TYPICAL PROCEDURE FOR THE SYNTHESIS OF 2- AND 4-IODO-5-[[4-[4-(DIISOBUTYLAMINO)BUTYL]-1-PHENYL]ACETYL]-10,11-DIHYDRO-5H-DIBENZO[B,E] [1,4]DIAZEPIN-11-ONES. 2-IODO-5-[[4-[4-(DIISOBUTYLAMINO) BUTYL]-1-PHENYL]ACETYL]-10,11-DIHYDRO-5H-DIBENZO[B,E][1,4]DIAZEPIN-11-ONE. Cohen et al., In preparation for J. Heterocyclic Chem.

8. SYNTHESIS OF 4-CHLOROALKYLPHENYLACETIC ACIDS AND 4-CHLOROALKYLCYCLOHEXYL-ACETIC ACIDS. Victor I. Cohen, Biyun Jin, and Richard C. Reba In preparation for Synthesis

9. FACILE AND GENERAL SYNTHESIS OF 2-, 3-, OR 4-[(DIALKYLAMINO) ALKYL]PYRIDINES AND PIPERIDINES. Victor I. Cohen, Biyun Jin, and Richard C. Reba, Liebigs Ann. Chem. 809-810, 1993.

PHARMACOLOGY

1. A NOVEL MUSCARINIC RECEPTOR LIGAND WHICH PENETRATES THE BLOOD BRAIN BARRIER AND DISPLAYS IN VIVO SELECTIVITY FOR THE m2 SUBTYPE. Miriam S. Gitler, Victor I. Cohen, Rosanna De La Cruz, Sheila F. Boulay; Biyun Jin, Barry R. Zeeberg, and Richard C. Reba. Life Sci. 53, 1743-1751.

2. [^{3}H]QNB DISPLAYS IN VIVO SELECTIVITY FOR THE m2 SUBTYPE. Miriam S. Gitler, Rosanna De La Cruz, Barry R. Zeeberg, and Richard C. Reba. Submitted to Life Sci.

3. SPECIFIC BINDING COMPONENT OF THE "INACTIVE" STEREOISOMER (S,S)-[^{125}I]IQNB TO RAT BRAIN MUSCARINIC RECEPTORS IN VIVO. S.F. Boulay, R.C. McRee, V.I. Cohen, V.K. Sood, B.R. Zeeberg, and R.C. Reba Submitted to Life Sci.

4. USE OF EX VIVO BINDING TO MEASURE THE BRAIN CONCENTRATIONS OF PUTATIVE RADIOLIGANDS. Jesse Baumgold, Pei-Ying Ling, and Richard C. Reba Nucl Med Biol, Int J Radiat Appl Instrum Part B, 19, 513-516,1992.

5. A NOVEL M2-SELECTIVE MUSCARINIC ANTAGONIST: BINDING CHARACTERISTICS AND AUTORADIOGRAPHIC DISTRIBUTION IN RAT BRAIN. Miriam S. Gitler, Richard C. Reba, Victor I. Cohen, Waclaw J. Rzeszotarski and Jesse Baumgold Brain Res., vol. 582, pp.253-260, 1992.

6. BINDING OF RADIOIODINATED SPECT LIGANDS TO TRANSFECTED CELL MEMBRANES EXPRESSING SINGLE MUSCARINIC RECEPTOR SUBTYPES. Zeeberg, Gitler, Baumgold, de la Cruz, and Reba. BBRC 179, 768-775, 1991.

7. KINETIC ANALYSIS OF RAT PAROTID GLAND MUSCARINIC RECEPTORS IN VIVO: COMPARISON WITH BRAIN AND HEART. Hiramatsu, Kawai, Reba, Simon, Baum, and Blasberg. Am. J. Physiol. 264, G541-552, 1993.

8. IN VIVO DISSOCIATION KINETICS OF [^{3}H]QUINUCLIDINYL BENZILATE: RELATIONSHIP TO MUSCARINIC RECEPTOR CONCENTRATION AND IN VITRO KINETICS. Gibson, Zeeberg, Melograna, Wang, Ruch, Braun, and Reba. Brain Res. 553, 110-116, 1991.

9. IN VIVO NONSPECIFIC BINDING PARAMETERS OF (R,R)-[^{125}I]4IQNB ESTIMATED FROM THE PHARMACOKINETICS OF THE (S,S)-[^{125}I]4IQNB STEREOISOMER (LETTER). Hertzman and Zeeberg. J. Cereb. Blood Flow Metab. 12, 173-176, 1992.

10. CONCERNING THE DISTRIBUTION OF CEREBRAL MUSCARINIC ACETYLCHOLINE RECEPTORS IN ALZHEIMER'S DISEASE (LETTER). Zeeberg. Arch. Neurol. 48, 1117-1118, 1991.

11. IN VIVO PHARMACOKINETIC SENSITIVITY OF [^{125}I]IQNB LOCALIZATION AS A REFLECTION OF MUSCARINIC ACETYLCHOLINE RECEPTOR CONCENTRATION IN RAT BRAIN. Miriam S. Gitler, Barry R. Zeeberg, Richard C. Reba, Rosanna A. de la Cruz, Christy S. John, and Victor I. Cohen. Submitted to Life Sci.

12. PHARMACOKINETIC SENSITIVITY OF IN VIVO (R,R)- AND (R,S)- [^{125}I]IQNB LOCALIZATION AS A FUNCTION OF AVAILABLE REGIONAL MUSCARINIC RECEPTOR CONCENTRATION. Miriam S. Gitler, Barry R. Zeeberg and Richard C. Reba. In preparation for Life. Sci.

13. MUSCARINIC RECEPTOR SELECTIVITIES OF 3-QUINUCLIDINYL 8-XANTHENECARBOXYLATE (QNX) IN RAT BRAIN. Raymond E. Gibson, Timothy A. Schneidau, Marion Gitler, Jesse Baumgold, Barry Zeeberg and Richard C. Reba. Life Sci, 54, 1757-1765, 1994.

IMAGING PHYSICS

1. 3D SPECT SIMULATIONS OF A COMPLEX 3D MATHEMATICAL BRAIN MODEL: EFFECTS OF DETECTOR RESPONSE, ATTENUATION, SCATTER, AND STATISTICAL NOISE. Hee-Joung Kim, Barry R. Zeeberg, Frederic H. Fahey, Edward J. Hoffman, and Richard C. Reba. IEEE Trans. Med. Imag., vol. 11, pp. 176-184, 1992.

2. COMPENSATION FOR 3-D DETECTOR RESPONSE, ATTENUATION, AND SCATTER IN SPECT GREY MATTER IMAGING USING AN ITERATIVE RECONSTRUCTION ALGORITHM WHICH INCORPORATES A HIGH RESOLUTION ANATOMICAL IMAGE. Hee-Joung Kim, Barry R. Zeeberg, and Richard C. Reba. J. Nucl. Med. vol. 33, pp. 1225-1234, 1992.

3. EVALUATION OF RECONSTRUCTION ALGORITHMS IN SPECT NEUROIMAGING: 1. COMPARISON OF STATISTICAL NOISE IN SPECT NEUROIMAGES WITH "NAIVE" AND "REALISTIC" PREDICTIONS. Hee-Joung Kim, Barry R. Zeeberg, and Richard C. Reba Phys. Med. Biol. 38, 863-880, 1993.

4. EVALUATION OF RECONSTRUCTION ALGORITHMS IN SPECT NEUROIMAGING: 2. COMPUTATION OF DETERMINISTIC AND STATISTICAL ERROR COMPONENTS. Hee-Joung Kim, Barry R. Zeeberg, and Richard C. Reba Phys. Med. Biol. 38, 881-895, 1993.

5. ITERATIVE RECONSTRUCTION ALGORITHM WHICH INCORPORATES A HIGH RESOLUTION ANATOMICAL IMAGE: SIMULTANEOUS CORRECTION FOR 3-D DETECTOR RESPONSE, ATTENUATION, AND SCATTER IN SPECT NEURORECEPTOR IMAGING. Hee-Joung Kim, Barry R. Zeeberg, Richard C. Reba. 1991 IEEE NSS Conference Record, vol. 2, pp. 1980-1985, 1992.

6. GREY AND WHITE MATTER SPECT NEUROIMAGE RECONSTRUCTION: ITERATIVE RECONSTRUCTION USING A HIGH RESOLUTION ANATOMICAL IMAGE TO CORRECT FOR 3-D DETECTOR RESPONSE, ATTENUATION, AND SCATTER. Hee-Joung Kim, Barry R. Zeeberg, and Richard C. Reba, 1992 IEEE NSS Conference Record, vol. 2, pp. 1002-1004, 1993.

7. EVALUATION OF NEUROSPECT RECONSTRUCTION ALGORITHMS: DETERMINISTIC AND STATISTICAL ERRORS. Hee-Joung Kim, Barry R. Zeeberg, and Richard C. Reba, 1992 IEEE NSS Conference Record, vol. 2, pp. 1153-1155, 1993.

KINETIC MODELING

8. PHARMACOKINETIC SIMULATIONS OF SPECT QUANTITATION OF THE M2 MUSCARINIC NEURORECEPTOR SUBTYPE IN DISEASE STATES USING RADIOIODINATED (R,R)4IQNB. B.R. Zeeberg, H.J. Kim, and R.C. Reba. Life Sci., vol. 51, pp. 661-670, 1992.

9. ESTIMATION OF RELATIVE REGIONAL NEURORECEPTOR CONCENTRATION BY EMISSION COMPUTED TOMOGRAPHY: THEORETICAL COMPARISONS OF USING A SINGLE LATE IMAGE OR A LATE PLUS EARLY IMAGE. Barry R. Zeeberg, Hee-Joung Kim, and Richard C. Reba. IEEE Trans. Med. Imag. 12, 497-508, 1993.

10. ESTIMATION OF RELATIVE REGIONAL NEURORECEPTOR CONCENTRATION BY PET OR SPECT: A SINGLE LATE IMAGE COMPARED WITH A LATE PLUS EARLY IMAGE. Barry R. Zeeberg, Hee-Joung Kim, and Richard C. Reba, 1992 IEEE NSS Conference Record, vol. 2, pp. 918-920, 1993.